wjert, 2023, Vol. 9, Issue 4, 66-85. Review Article ISSN 2454-695X

World Journal of Engineering Research and Technology

WJERT

www.wjert.org

SJIF Impact Factor: 5.924

MODELING THE INTEGRATION OF AUTOMATIC GENERATION CONTROL (AGC) AND FACTS DEVICES TO IMPROVE GENERATION BALANCE AND STABILITY OF THE NIGERIA 330KV POWER GRID

Agwu, Emmanuel Anayo[1]*, Rufus Ogbuka Chime[2] and I. I. Eneh[3]

[1]Dept. of Electrical and Electronic Engineering Enugu State University of Science and Technology Enugu, Enugu State.

[2]Institute of management and Technology (IMT) Enugu.

[3]Enugu State University of Science & Technology Enugu, Nigeria.

Article Received on 03/02/2023 **Article Revised on 24/02/2023** **Article Accepted on 17/03/2023**

***Corresponding Author**
Agwu, Emmanuel Anayo
Council for the Regulation of Engineering in Nigeria (COREN), Port Harcourt, Rivers State.
agwuanayo@yahoo.com

ABSTRACT

When there is poor regulation in any interconnected power system, it is reflected in the buildup of time error and abnormal or unintended power flow over tie-lines. In remote systems, time error is of great concern. The error, which can hasten or slow the clocks, thereby resulting in a loss of load that can be billed, is reduced or adjusted by offsetting the scheduled frequency from the wanted value for a given period of time. An Imbalance between the electrical load and the power supplied by the connected generators is a direct result of frequency deviation. The strategy used here for the integration is to model a neural network controller for controlling UPFC for the injection and adsorption of active and reactive power into the tie-line to maintain power balance via power electronics. This would modulate the power flow between the areas through the tie-line, especially in the event of load and generation disturbances in the controlled areas of the interconnected power system Power flow UPFC model contains two voltage source converters (VSC), one has shunt connection and the other has series connection. The converters have DC capacitors, which are connected in parallel. When switches, 1 and 2 are open, the converters are STATCOM and SSSC, governing the injected reactive current and voltage in shunt and series of the line. Closing switches 1 and 2 enables the two converters to

transfer real power. The series connected converter can draw or generate the active power. The objective for this work is to model the integration of AGC and FACTS devices on the tie-line in the two area interconnected power system to control power flow. , this study proposes the use of software to improve generation balance of the 330KV Power Grid by integrating AGC-FACTS devices. Modeling of the UPFC power flow, initialization & dynamic modeling of the UPFC controller are vital in the modeling of the neural network for the control of the UPFC. Results obtained from the simulations carried out with the UPFC integrated into the tie – line of the interconnected power system shows improvement of the time error and ACE reduction curve following the load disturbance.

KEYWORDS: *FACT Devices, Automatic Generation Control, Unified Power Flow Controller, Neural Network Controller and Tie-Lie.*

INTRODUCTION

Automatic Generation Control provides all the necessary mechanism for the adjustment of power generation to reduce frequency deviation and regulate tie-line power flows. The system realizes generation changes by sending control signals to the generating units on the power grid. In summary, the AGC performance depends very much on how each of those generating units respond to the commands.

An Imbalance between the electrical load and the power supplied by the connected generators is a direct result of frequency deviation. Therefore, it helps to provide a useful index to indicate the generation and load imbalance. Frequency deviation directly impacts on power system operation, security, reliability, and efficiency by damaging equipment, degrading load performance, overloading transmission lines, and triggering the protection devices.

FACTS devices are excellent for the control of power since they are based on power electronics. The AGC maintains frequency and tie-line power flow by controlling generation. The concept of integrating FACTS devices and AGC system is to leverage on the finer control that FACTS devices can provide for the control of power flow on the tie-line interconnecting the areas in the interconnected power system. The most popular conventional controller used with FACTS devices is the proportional integral controller. Due to the complexity integrating AGC output control signal and from the controller areas, parameters for transmission loss reduction (the tie-line being a transmission line, loss reduction is vital to ensuring power balance in all the areas), parameters to ensure power and frequency balance

in the interconnected power system, a neural network is modeled and trained in this work for the control of the integrated FACTS device. The FACTS device integrated in this work is the Unified Power Flow Controller (UPFC).

UPFC is a combination of static synchronous compensator (STATCOM) and a static synchronous series compensator (SSSC). They are joined through a common dc link, to allow bi-directional flow of real power between the series output terminals of the SSSC and the shunt output terminals of the STATCOM. They are controlled to provide concurrent real and reactive series line compensation without an external electric energy source. (Mohamed Zellagui & Abdelaziz Chaghi, 2013). The UPFC, by means of angularity unconstrained series voltage injection is able to control concurrently or selectively, the tie-line power flow, voltage, impedance, and angle or alternatively, the real and reactive power flows in the tie-line.

The scheme used here for the integration of the UPFC is to model a neural network controller for controlling UPFC for the injection and adsorption of active and reactive power into the tie-line to maintain power balance via power electronics. This would modulate the flow of power between the area 1 and area 2 via the tie-line, particularly in the event of load and generation disturbances in the controlled areas of the interconnected power system. Modeling of the UPFC power flow, initialization & dynamic modeling of the UPFC controller are vital in the modeling of the neural network for the control of the UPFC.

Literature review

Arya et al (2020) carried out studies on AGC performance amelioration in multi-area interconnected thermal and thermal-hydro-gas power systems using a novel controller. In the work carried out, a novel cascade fuzzy-proportional integral derivative incorporating filter (PIDN)-fractional order PIDN (FPIDN-FOPIDN) controller was offered as an expert control strategy to deal effectively with AGC issue of interconnected power systems (IPS). Imperialist competitive algorithm was prolifically utilized for optimizing the controller parameters. Initially, a two area non-reheat thermal IPS was studied in detail and next to attest the efficacy of the technique, the study was extended to realistic two-area multi-source thermal-hydro-gas and reheat thermal three-area systems. The power systems used in the work were interconnected two-area non-reheat thermal (TANRT), realistic multisource two-area thermal-hydro-gas (MSTATHG) and unequal three-area reheat thermal (TART) power systems. The TANRT system has one non-reheat type of turbine and TART system involves

of one single reheat type of turbine in individual area. The MSTATHG system consists of one reheat thermal, one hydro (mechanical governor) and one gas generating units in each control area. Ratings of each area of TANRT and MSTATHG systems used is 2000 MW. TART system has ratings of area-1, area-2 and area-3 as 2000 MW, 5000 MW and 8000 MW, in order. A biasing B = b was contemplated in each area. MATLAB/ SIMULINK R2015b was employed for coding, models and results of the systems. The TANRT power system was simulated under a step load perturbation (SLP) of 5% pu MW in area-1 (DPD1 = 0.05 puMW) at t = 0 s employing PIDN, FPIDN and FPIDN-FOPIDN controllers. The parameters of FPIDN and FPIDN-FOPIDN controllers were obtained by means of ICA. From simulations carried out, power system dynamic responses of change in area-1 frequency (DF1), change in area-2 frequency (DF2) and change in power of tie-line (DPtie12) were presented graphically. To manifest the dominance of cascade FPIDN-FOPIDN controller, its responses were equated with some existing control methods emerged recently in the literature such as PIDN controller tuned via jaya algorithm (JA) (Sugandh et al, 2017), fuzzy PI (FPI) controller tuned via PSO (particle swarm optimization)/PS (pattern search/hPSO-PS (hybrid PSO-PS) (Rabindra et al, 2015), FPID controller adjusted via hHS-COA (hybrid harmony search-cuckoo optimization algorithm) (Meysam Gheisarnejad, 2018)/hIFA-PS (hybrid improved firefly algorithm-PS) (Rajesh, Dash & Rajagopal, 2019), FPIDN controller tuned via hLUS-TLBO (hybrid local unimodal sampling-teaching learning based optimisation) and ICA tuned PIDN/FPIDN controllers. Findings from results obtained showed that the offered cascade FPIDN-FOPIDN controller provides superior outcomes compared to other controllers regarding improved and fast oscillation free responses showing no over shoots and trivial peak under shoots. The superiority of the ICA optimized FPIDN-FOPIDN over ICA optimized FPIDN and ICA optimized PIDN controllers was also exposed from their convergence outcomes. This demonstrates that the cost function (J) i.e., ISE value corresponding to FPIDN-FOPIDN is smaller compared to FPIDN/PIDN. Moreover, FPIDN-FOPIDN controller was determined to converge faster compared to FPIDN/ PIDN controller. The authors showed, from the results obtained, FPIDN-FOPIDN controller are smooth with lowest US/OS/JS and correctly reach to the preferred zero steady state values in minimum time under a step load change (SLP) in a control area compared to JA /ICA: PIDN, PSO/PS/hPSO-PS: FPI, hHS-COA [25]/hIFA-PS : FPID and ICA/hLUS-TLBO : FPIDN controllers. Hence, it was concluded that the proposed controller demonstrated better dynamic performance in AGC of the power systems industry.

Yogendra Arya (2018) presented an output scaling factor (SF) based fuzzy classical controller to enrich AGC conduct of two-area electrical power systems. In the work carried, an implementation of imperialist competitive algorithm (ICA) was made to optimize the output SF of fuzzy proportional integral (FPI) controller employing integral of squared error criterion. The study was conducted on a well-accepted two-area non-reheat thermal system with and without considering the appropriate generation rate constraint (GRC). Two power system models were investigated. First system is a non-reheat thermal system. Each area of two-area non-reheat thermal system consists of one non-reheat type thermal turbine and one governor. The second system is a two-area reheat thermal-photo voltaic (PV) system having PV plant in area-1 and reheat thermal plant with governor in area-2. Simulations were carried out to validate the work.

The simulation results were obtained with 1% and 5% step load change (SLP) in area-1 at $t = 0$ s. The study was further extended to the two-area reheat thermal-PV grid system under 10% SLP in area-2 and 10%.

The advantage of the proposed controller was illustrated by comparing the results with fuzzy controller and bacterial foraging optimization algorithm (BFOA)/genetic algorithm (GA)/particle swarm optimization (PSO)/hybrid BFOA-PSO algorithm/firefly algorithm (FA)/hybrid FA-pattern search (hFA-PS) optimized PI/PID controller prevalent in the literature. In the validation carried out, the superiority of the method was depicted by contrasting the results of GA/FA tuned PI controller. The proposed control approach was also implemented on a multi-unit multi-ource hydrothermal power system and its advantage was established by correlating its results with GA/hFA-PS tuned PI, hFA-PS/grey wolf optimization (GWO) tuned PID and BFOA tuned FPI controllers. Finally, a sensitivity analysis was performed to demonstrate the robustness of the proposed method to broad changes in the system parameters and size and/or location of step load perturbation. With regards to gaps found in the research; considering that the work concerned multi-area interconnected power system, the authors did not evaluate the impact of the proposed AGC system on Area Control Error (ACE) and on tie-line power interchange.

Gupta, Kar & Singh (2022) proposes an improved sine–cosine algorithm (ISCA) based degree of freedom proportional integral derivative (2-DOF-PID) controller for load frequency control. In the work carried out, the authors used the ISCA method to tune the controller of load frequency control (LFC) i.e the AGC system. The 2-DOF-PID controller based on ISCA

was designed and implemented for LFC of a three-area power system with and without nonlinearities, and then further applied to a four-area power system. The objective function used is integral of time-weighted absolute error (ITAE), and by minimizing the ITAE. A three-area system was considered for the case study. The system is an unequal system that consists of three thermal generators having different parameter values. In each area, there are governor, turbine, generation and load sections. To validate the effectiveness of the proposed method, the ISCA is applied for the tuning of the LFC controller parameters. The communication delay of 40 ms, GDB of 0.036 pu, and GRC of 3% pu are considered in each area of the system. The 2-DOF-PID controlled test system was simulated when disturbances of 2% was applied in area-1 and area-2. The comparison was carried out with recently used algorithms of Particle swarm optimization (PSO), Salp swarm algorithm (SSA), Sine–cosine algorithm (SCA), and Ant-lion optimization (ALO). Graphically (convergence curves) showed that the ISCA achieves the lowest objective function (ITAE value) and converges faster than the other methods. The different performance parameters such as peak undershoot, settling time of frequency and tie-line power were improved. It was concluded from the convergence curve, dynamic response, and performance parameters that the proposed ISCA method has much better tuning efficiency than other optimization methods. The ISCA was found to perform much better than the other optimization techniques. However, considering that the key function of the ISCA was tuning of the controller, the work has the downside that the authors did not consider the generator governor dead band in the tuning of the controller.

Sahu, P.C., Prusty, R.C. & Sahoo, B.K (2020) carried out research presenting the implementation of a fuzzy rule and membership function-based fuzzy-aided PID controller for automatic generation control (AGC) in multi-area nonlinear power system. At the initial stage of this proposed work, a three-area nine-unit installed interconnected network was considered for developing different dynamic responses in response to AGC analysis. A modified approach named modified sine cosine algorithm (M-SCA) was proposed for tuning the gain parameters of the above-proposed fuzzy controller to produce close optimum gain values. The proposed modified algorithm was developed from its original sine cosine algorithm by improving and updating few equations which is capable of making the balance between exploration and exploitation levels of this algorithm and improving the updating quality of iteration. To impose supremacy of M-SCA technique, it was examined through convergence curves and its performance was compared with host sine cosine algorithm, genetic algorithm, and particle swarm optimization algorithm. For controller supremacy analysis, the performance of the proposed fuzzy-aided PID controller was compared with

conventional integral(I), proportional integral(PI), and Proportional Integral Derivative(PID) controllers, and it has been revealed that proposed M-SCA-tuned fuzzy-aided PID controller exhibits better performances through different deviated responses for AGC analysis. To demonstrate most standard and supremacy of the proposed approaches, simulations and evaluation was carried out through a five-area ten-unit system considering some physical nonlinear constraints like generation rate constraint, governor dead band, boiler dynamics and time delay. At the final observation level, the proposed fuzzy controller has gone through different sensitivity analyses with variation of different system parametric conditions and different load conditions. However, the authors did not model how the fuzzy logic systems membership could be used to tune the PID controller.

Rabindra et al (2017) presented the design and analysis of differential evolution algorithm based automatic generation control for interconnected power system. The schemes used are Differential Evolution (DE) algorithm and Proportional-Integral-Derivative (PID) controller. Authors worked on the design and performance analysis of Differential Evolution (DE) algorithm based parallel 2-Degree Freedom of Proportional-Integral-Derivative (2-DOF PID) controller for Load Frequency Control (LFC) of interconnected power system. DE is employed to search for optimal controller parameters. Work was validated using simulations. Proposed controller reduced controller settling time by 6.23%. It achieved a reduction in ACE of about 13.65% and reduction in frequency deviation of about 10.76% compared to PID controller. The proposed controller was validated with a wide variation in systems load. However, the processor cycle required to compute the control load increased with increase in load variation. A reported limitation of DE is that it, "easily drop into the optimum region "which can be overcome by a novel DEPSO algorithm in DE and Particle Swarm Optimization (PSO). The downsides of the work includes that the authors did not take generation economic dispatch to consideration and impact of integration of controller with modern compensation devices like FACTS was not evaluated.

Ali & Abd-Elazim (2018) carried out work in AGC. The work carried out focused on Artificial Intelligence based technique, the Bacterial Foraging Optimization Algorithm (BFOA) for the suppression of oscillation and optimize the integral plus double derivative (IDD) controller in the power system consists of two, three and five unequal areas non-reheat thermal system equipped with proportional plus integral (PI) and IDD controllers. Numerical results indicated in comparison with PID, the proposed controller achieved a 5.2% reduction

in settling time, a 16.87% reduction in tie-line power flow deviation, a 12.45% reduction in frequency deviation. However, the authors work did not evaluated the effect of abrupt inter area power interchange on the stability of the power system.

Praghnesh Bhatt (2017) carried out optimized multi area AGC simulation in restructured power systems‖ Electrical Power and Energy Systems using Hybrid particle swarm Optimization. In the work carried out by the authors, automatic generation control loop with modifications is integrated in simulating automatic generation control (AGC) in modernized power system is presented. Hybrid particle swarm optimization to attain optimal gain parameters for optimal transient performance. Result obtained showed slight reduction in frequency deviation and ACE. However gaps can be observed in the work. The authors did not validate the solution under random load variation and the scheme only worked well for only a two area interconnected power system. It proposed inconsistent result with multi area interconnected power system of more than two areas.

Santigopal et. al (2018) carried out work on AGC titled Multi-objective Optimization of Load Frequency Control using PSO. The methodology involved the usage of Particle swarm optimization & PID. Work carried was on a practical model for load frequency control (LFC) of two-area interconnected power system. A PID controller is used for the design and analysis of the proposed model and PSO is applied to obtain suitable control parameters to achieve the optimum performance. Simulations was used to validate the work. The proposed hybrid controller achieved a reduction of 8.76% reduction in tie-line power deviation in comparison only PSO and 21.33% tie-line power deviation in comparison with only PID. The proposed controller was validated with a wide variation in systems load. However, the convergence of the hybrid algorithm was slow. Other downsides of the work include that the authors did not integrate economic load dispatch in the specification of the PSO objective function. Furthermore system loss validate system under loss of generator contingency and large load drops.

1. Modelling the UPFC Power Flow

Power flow UPFC model contains two voltage source converters (VSC), one has shunt connection and other has series connection. The converters have DC capacitors, which are connected in parallel as shown in Figure 1. When switches, 1 and 2 are open, the converters are STATCOM and SSSC, governing the injected reactive current and voltage in shunt and

series of the line. Closing switches 1 and 2 enables the two converters to transfer real power. The series connected converter can draw or generate the active power.

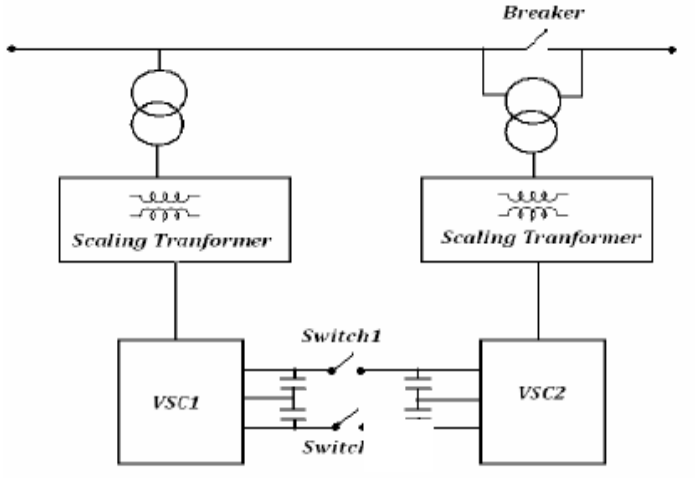

Figure 1: A UPFC schematic.

The general transfer admittance matrix is obtained by applying Kirchhoff current and voltage laws to the electric circuit shown in Figure 2.

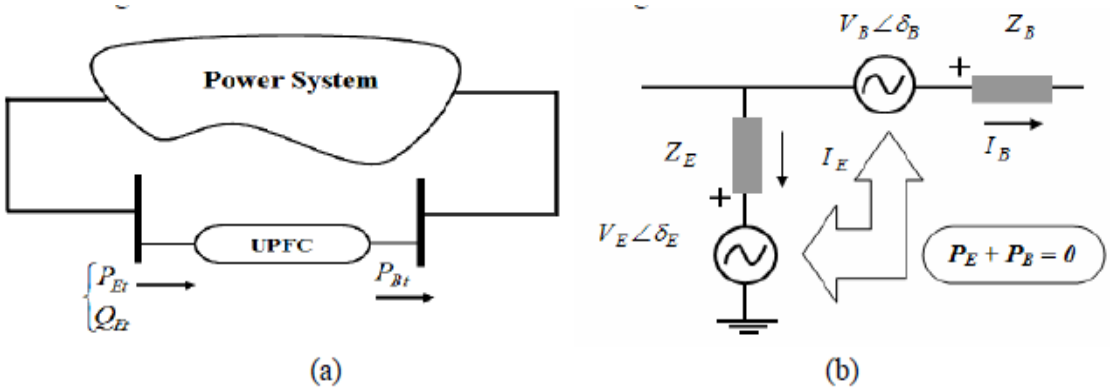

Figure 2: (a) UPFC Power Flow Model (b) UPFC Single Line Diagram.

Considering the sending shunt bus *k* and the receiving series bus *m*, and writing the injected currents at *m* and *k* buses (Zellangui, 2017):

$$\begin{bmatrix} I_k \\ I_m \end{bmatrix} = \begin{bmatrix} y_B + y_E & -y_B & -y_B & -y_E \\ -y_B & y_B & y_B & 0 \end{bmatrix} \begin{bmatrix} V_k \\ V_m \\ V_B \\ V_E \end{bmatrix} \quad \ldots\ldots\ldots\ldots\ldots\ldots\ldots\ldots\ldots\ldots (1)$$

$$\Delta Y_{bus} = \begin{bmatrix} Y_{kk} & Y_{km} & Y_{kB} & Y_{kE} \\ Y_{mk} & Y_{mm} & Y_{mB} & 0 \end{bmatrix} \quad \text{...} (2)$$

The original *Ybus* of the system before installing the UPFC is modified to include the UPFC model by adding Δ*Ybus* to it, and in this case the number of columns of the new *Ybus* will be increased by two corresponding to *VB* and *VE*.

Considering a lossless converter operating, the UPFC will not draw nor supply real power with respect to the network. The real power demanded by the series converter is supplied from the network by the shunt converter via the common DC link voltage. The DC link voltage, *Vdc*, must remain constant so that the stored energy in the capacitor would not be changed. Hence, the active power supplied to the shunt converter, *PE*, must satisfy the real power demanded by the series converter, *PB*:

$PE + PB = 0$………………………. (3)

Where

$$\begin{aligned} P_B &= -real(V_B^* I_B) = -real(V_B^*(V_k - V_m - V_B)Y_{mB}) \\ &= V_B^2 G_{mB} - V_B Y_{mB} V_k \cos(\theta_{mB} + \delta_k - \delta_B) + V_B Y_{mB} V_m \cos(\theta_{mB} + \delta_m - \delta_B) \end{aligned} \quad \text{...........} (4)$$

$$\begin{aligned} P_E &= -real(V_E^* I_E) = -real(V_E^*(V_k - V_E)(-Y_{kE})) \\ &= -V_E^2 G_{kE} + V_E Y_{kE} V_k \cos(\theta_{kE} + \delta_k - \delta_E) \end{aligned} \quad \text{.......................................} (5)$$

$$\begin{aligned} P_B + P_E &= V_B^2 G_{mB} - V_E^2 G_{kE} - V_B Y_{mB} V_k \cos(\theta_{mB} + \delta_k - \delta_B) \\ &\quad + V_B Y_{mB} V_m \cos(\theta_{mB} + \delta_m - \delta_B) + V_E Y_{kE} V_k \cos(\theta_{kE} + \delta_k - \delta_E) \end{aligned} \quad \text{.........} (6)$$

The UPFC linearized power equations are combined with the linearized system equations corresponding to the rest of the network

$$[\Delta f(x)] = [J][\Delta x] \quad \text{...} (7)$$

Where

$$[\Delta f(x)] = [\Delta P_k \ \Delta P_m \ \Delta Q_k \ \Delta Q_m \ \Delta P_{mk} \ \Delta Q_{mk} \ \Delta(P_B + P_E)] \quad \text{.........................} \ (8)$$

$[\Delta x]$ is the solution and $[J]$ is the Jacobian matrix.

2. Effective Initialization of the UPFC Controllers

For the UPFC to be effectively controlled for the control of tie-line power flow (with the aide of loss minimization) , the initialization of the parameters of the converters (The series and shunt converters) within power flow solutions(e.g. the Newton-Raphson power flow solution) is necessary. The modeling of UPFC controllers for applications such as controlling tie-line power flow involving power flow analysis results in highly nonlinear equations, which should be suitably initialized to ensure quadratic convergent solutions when using the Newton–Raphson method.

Extensive application of FACTS devices represented by shunt voltage sources shows that elements such as the STATCOM, the shunt source of the UPFC, and the two-shunt sources representing the HVDC-VSC are suitably initialized by choosing 1 p.u. voltage magnitudes and 0 phase angles.

Suitable initialization of series voltage sources in load flow analysis is obligatory to guarantee robust solutions. Different equations exist for the purpose of initializing the series voltage source of the UPFC, depending on the operating condition exhibited by the controller. For the case when active and reactive powers are specified at bus *k*, and assuming

$V_k = V_m = 1$ p.u., and $\theta_k = \theta_m = 0$, leads to the following simple expression

$$V_B = V_{cR} = X_B (P^2_{specified} + Q^2_{specified})^{1/2} \quad \text{...} \ (9)$$

$$\theta_E = \theta_{cR} = \arctan\left(\frac{P^2_{specified}}{Q^2_{specified}}\right) \quad \text{...} \ (10)$$

These equations are used to initialize the parameters of series voltage sources within the Newton–Raphson power flow solution. The flow chart shows the general load flow algorithm with UPFC.

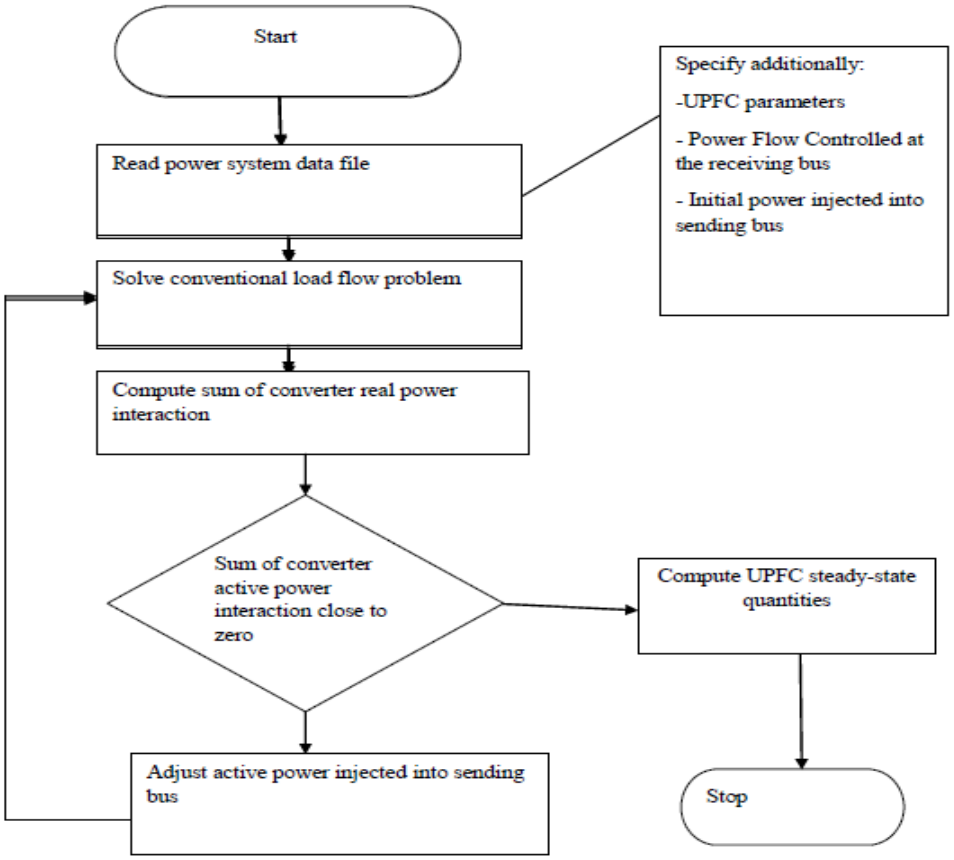

3. Dynamic Modelling of the UPFC

Figure 3 shows the UPFC schematic description. The two converters in the schematic own the same construction, but is varied in their rated values. The network voltages (magnitude, angles) of the two converters output can be updated according to the operating requests of the system.

Therefore, there are four control inputs: *mE*, *mB* and δE, δB, that are the amplitude modulation ratio and phase angle of the control signal of each VSC, as shown in Figure 3.

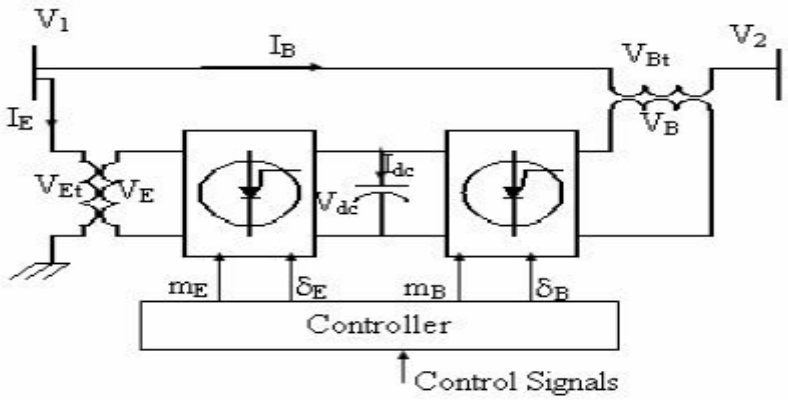

Figure 3: Schematic diagram of the power circuit of a UPFC.

An equivalent UPFC model, which is based on the Pulse Width Modulation (PWM) approach, is shown in Figure 4.

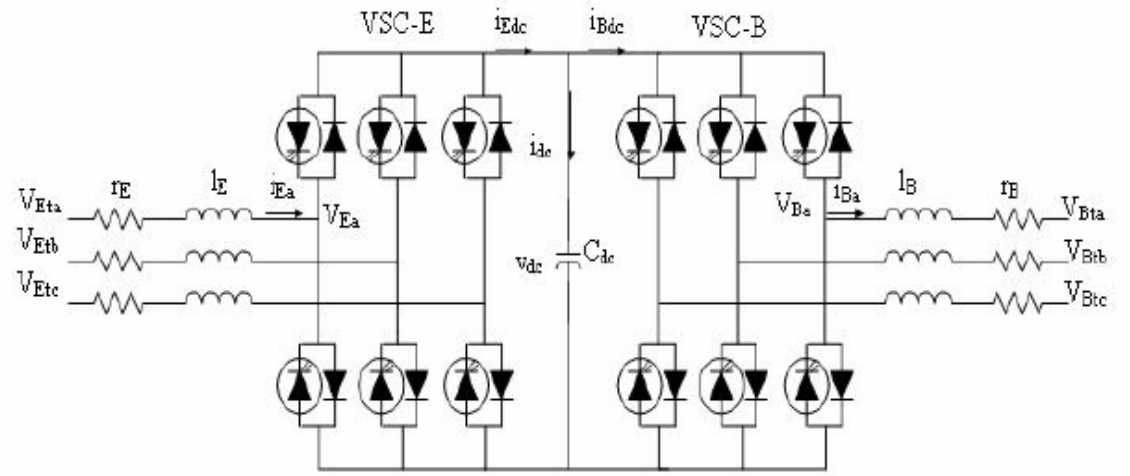

Figure 4: Equivalent UPFC Model.

The three-phase differential equations of the UPFC are:

$$\begin{bmatrix} \frac{di_{Ea}}{dt} \\ \frac{di_{Eb}}{dt} \\ \frac{di_{Ec}}{dt} \end{bmatrix} = \begin{bmatrix} -\frac{r_E}{l_E} & 0 & 0 \\ 0 & -\frac{r_E}{l_E} & 0 \\ 0 & 0 & -\frac{r_E}{l_E} \end{bmatrix} \begin{bmatrix} i_{Ea} \\ i_{Eb} \\ i_{Ec} \end{bmatrix} + \begin{bmatrix} \frac{1}{l_E} & 0 & 0 \\ 0 & \frac{1}{l_E} & 0 \\ 0 & 0 & \frac{1}{l_E} \end{bmatrix} \begin{bmatrix} v_{Eta} \\ v_{Etb} \\ v_{Etc} \end{bmatrix} - \begin{bmatrix} \frac{1}{l_E} & 0 & 0 \\ 0 & \frac{1}{l_E} & 0 \\ 0 & 0 & \frac{1}{l_E} \end{bmatrix} \begin{bmatrix} v_{Ea} \\ v_{Eb} \\ v_{Ec} \end{bmatrix} \quad \text{.....(11)}$$

$$\begin{bmatrix} \frac{di_{Ba}}{dt} \\ \frac{di_{Bb}}{dt} \\ \frac{di_{Bc}}{dt} \end{bmatrix} = \begin{bmatrix} -\frac{r_B}{l_B} & 0 & 0 \\ 0 & -\frac{r_B}{l_B} & 0 \\ 0 & 0 & -\frac{r_B}{l_B} \end{bmatrix} \begin{bmatrix} i_{Ba} \\ i_{Bb} \\ i_{Bc} \end{bmatrix} + \begin{bmatrix} \frac{1}{l_B} & 0 & 0 \\ 0 & \frac{1}{l_B} & 0 \\ 0 & 0 & \frac{1}{l_B} \end{bmatrix} \begin{bmatrix} v_{Bta} \\ v_{Btb} \\ v_{Btc} \end{bmatrix} - \begin{bmatrix} \frac{1}{l_B} & 0 & 0 \\ 0 & \frac{1}{l_B} & 0 \\ 0 & 0 & \frac{1}{l_B} \end{bmatrix} \begin{bmatrix} v_{Ba} \\ v_{Bb} \\ v_{Bc} \end{bmatrix} \quad \text{....(12)}$$

Where V_E, V_B and V_{dc} are given by:

$$\begin{bmatrix} v_{Ea} \\ v_{Eb} \\ v_{Ec} \end{bmatrix} = \frac{\sqrt{2} m_E v_{dc}}{2} \begin{bmatrix} \cos(\omega t + \delta_E) \\ \cos(\omega t + \delta_E - 120^0) \\ \cos(\omega t + \delta_E + 120^0) \end{bmatrix} \quad \text{.....(13)}$$

$$\begin{bmatrix} v_{Ba} \\ v_{Bb} \\ v_{Bc} \end{bmatrix} = \frac{\sqrt{2} m_B v_{dc}}{2} \begin{bmatrix} \cos(\omega t + \delta_B) \\ \cos(\omega t + \delta_B - 120^0) \\ \cos(\omega t + \delta_B + 120^0) \end{bmatrix} \quad \ldots\ldots\ldots\ldots(14)$$

V_E and V_B can be written as phasor quantities

$$V_E = \frac{m_E v_{dc}}{2} \angle \delta_E \quad \ldots\ldots\ldots\ldots..(15)$$

$$V_B = \frac{m_B v_{dc}}{2} \angle \delta_B \quad \ldots\ldots\ldots\ldots(16)$$

$$\frac{dv_{dc}}{dt} = \frac{m_E}{2C_{dc}}[\cos(\omega t + \delta_E) i_{Ea} + \cos(\omega t + \delta_E - 120^0) i_{Eb} + \cos(\omega t + \delta_E + 120^0) i_{Ec}]$$
$$+ \frac{m_B}{2C_{dc}}[\cos(\omega t + \delta_B) i_{Ba} + \cos(\omega t + \delta_B - 120^0) i_{Bb} + \cos(\omega t + \delta_B + 120^0) i_{Bc}] \quad \ldots\ldots(17)$$

4. The model of the UPFC Neural network controller

The strategy for ensuring power balance is the intelligent control of the FACTS device in order to put under control the power flow through the tie-line from one control area to another control. The shunt and series controllers of the UPFC for the control of reactive power injection into or absorption from the tie-line in the events of generation or load disturbances. The neural network control is to generate the right levels of amplitude modulation ratios (*mE*, *mB)* and phase angles (i.e firing angles δE, δB,) of the control signal of each VSC in the UPFC. Figure 5 shows the functional model of the UPFC with the neural network controller.

For the control of the UPFC for the injection of the right active and reactive power in order to adapt the transmission system power flow for power balance two neural network controllers are used: One for the control of the series VSC and the other for the control of the shunt VSC.

The neuro-controller model is a multi-layer feed-forward network trained with Modified Recursive Prediction Error Algorithm (MRPE).

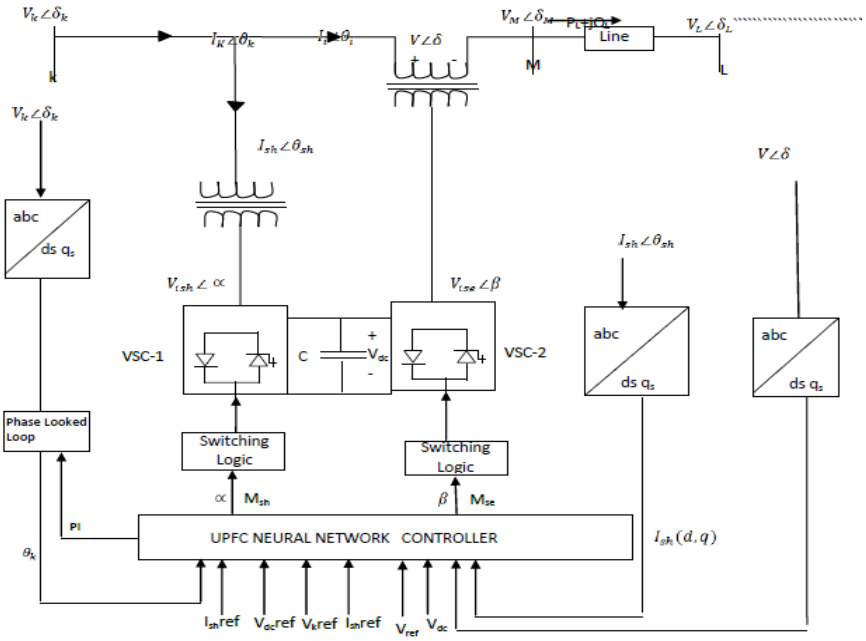

Figure 5: The UPFC Functional model.

The neural network controls the injection of real and reactive power by the UPFC into the tie -line current, voltage and impedance are put under control in order to modulate the power flow. The main objective of the series **converter** is to produce an ac voltage of controllable magnitude and phase angle, and inject this voltage at fundamental frequency into the transmission line, exchanging real and reactive power at its ac terminals through the series connected transformer. The shunt converter provides the required real power at the dc terminals; thus, real power flows between the controller shunt and series ac terminals through the common dc link.

Inputs to the UPFC series Neural Network Controller:

- Shunt converter (i.e. shunt VSC) reference current: $I_{sh_{ref}}$
- Link capacitor reference voltage:$V_{dc_{ref}}$
- ACE1 and ACE2
- ΔPD_1 and ΔPD_2
- Operating voltage reference: V_{ref}
- Active power injected at node j: P_j
- Reactive power injected at node j: Q_j
- Active loss at the i^{th} and $(i+1)th$ bus: $P_{loss\ i,i+1}$

- Power balance deviation: P_{dev}
- Minimum voltage constraint deviation: $V_{min_{dev}}$
- Maximum voltage constraint deviation: $V_{max_{dev}}$

Output of the UPFC series neural network controller:

- amplitude modulation ratio : *mE*
- firing angle: δE

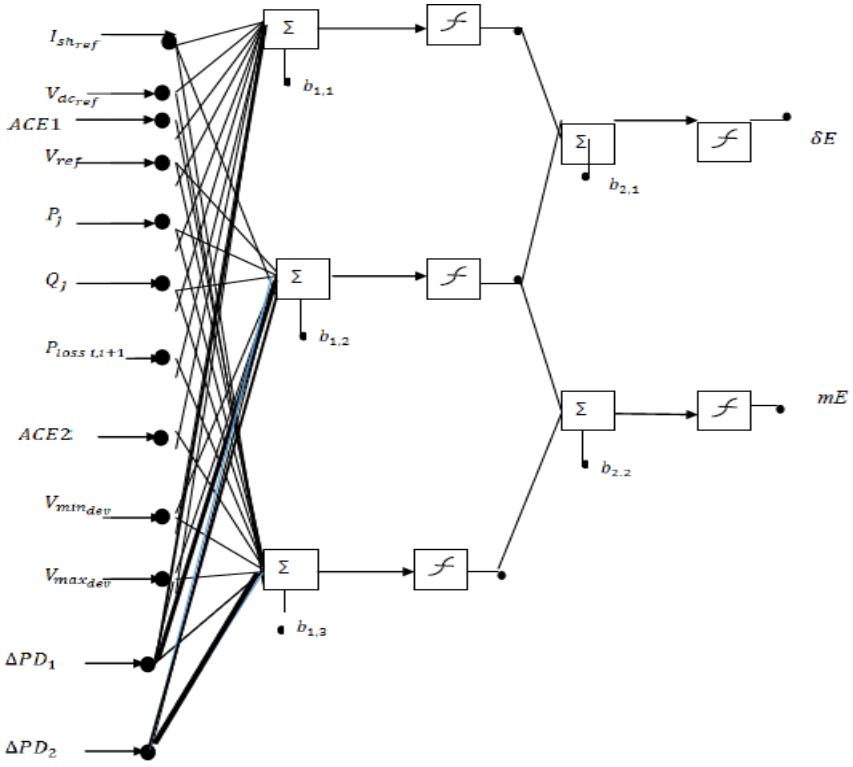

Figure 6: Model of the neural network controller for the tie-line power control UPFC.

5. Evaluation of the impact of the FACTS device on the tie – line.

Results obtained from the simulations carried with the UPFC integrated into the tie – line of the interconnected power system having the RNN-MPC AGC system shows further improvement of the time error and ACE reduction trajectory following the load disturbance. Figure 7 shows the time error with and without the UPFC installed on the tie – line.

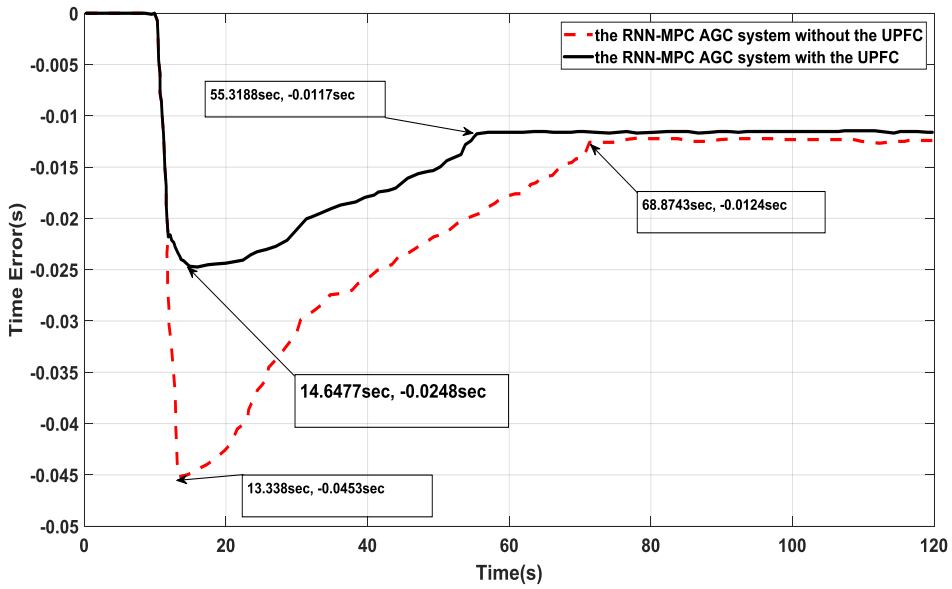

Figure 7: Time error of the power system for the proposed AGC system With and Without the installation of the UPFC.

It can be observed from the graph that, with the presence of the UPFC, the time error was restored to steady state in a very short time. The use of the RNN- MPC AGC system with the UPFC on the tie – line restored the time error to steady state in about 45.3188 seconds following the system perturbation. This is less than the time it took with the RNN – MPC system without UPFC.

Furthermore, it can be noticed that with the integration of the UPFC, the accumulation of time error increased to about – 0.0242 seconds, whereas without the RNN-MPC AGC system it increased to –0.0493 seconds (I.e., increased to a greater value a little more than twice the formal value). This shows that the UPFC even began to process rebalancing of the grid probably even before supplementary control might have been activated. The UPFC suppressed the drift or large deviations in the time error. The result obtained shows that the integration of UPFC reduced the accumulation of time error by about 50.91%.

6. CONCLUSION

Frequency deviation is a direct result of the imbalance between energy supply and demand (i.e. imbalance between the electrical load and the power supplied by the connected generators in the power system). This imbalance affects power system operation, security, reliability, and efficiency by damaging equipment, degrading load performance, overloading transmission lines, and triggering the protection devices. Since transmission systems provide

negligible energy storage, energy supply and demand must be balanced by either generation or load control. This is why AGC is very vital. In conclusion, it is very vital to continue to research on modern and smart techniques for the improvement or enhancements of AGC in modern power systems. This work showed that the integration of FACTS devices can be considered for the enhancements and modernization of AGC systems in interconnected power systems.

7. REFERENCES

1. J. Kumar, K. H. Ng, and G. Sheble, "AGC simulator for price-based operation, part 1: A model," *IEEE Transactions on Power Systems*, 1997; 12, 2: 527–532.
2. M. Scherer, E. Iggland, A. Ritter, and G. Andersson, "Improved frequency bias factor sizing for non-interactive control," in Presented at the Cigre session, Paris, France, 2012; 44.
3. K. S. S. Ramakrishna, Pawan Sharma, T. S. Bhatti ― Automatic generation control of interconnected power system with diverse sources of power generation‖ International Journal of Engineering, Science and Technology, 2010; 2, 5: 51-65.
4. H. Golpira, H. Bevrani ―Application of GA Optimization for Automatic Generation Control in Realistic Interconnected Power Systems" Proceedings of the International Conference on Modelling, Identification and Control, Okayama, Japan, 2010; 17-19.
5. Z. Al-Hamouz, H. Al-Duwaish, N. Al-Musabi ―Optimal design of a sliding mode AGC controller: Application to a non-linear interconnected model" Z. Al-Hamouz et al. / Electric Power Systems Research, 2011; 81: 1403–1409.
6. Poonam Singhal, Taransum Bano ― Automatic Load Frequency Control of Two-area interconnected Thermal Reheat Power System using Genetic Algorithm with and without GRC" International Journal of Engineering Research and General Science, 2015; 3: 2. ISSN 2091-273.
7. Rabindra Kumar Sahu, Sidhartha Panda, Umesh Kumar Rout "Design and analysis of differential evolution algorithm based automatic generation control for interconnected power system" Ain Shams Engineering Journal, 2013; 4: 409–421.
8. Rekhasree R L, J.Abdul Jaleel ―Automatic Generation Control of Complex Power Systems Using Genetic Algorithm: A case Study‖ International Journal of Engineering Research & Technology (IJERT), 2013; 2: 10.
9. Tulasichandra Sekhar Gorripotu, Rabindra Kuma r Sahu, Sidhartha Panda―DE Optimized PID Controller with Derivative Filter for AGC of Interconnected Restructured

Power System" H.S. Behera and D.P. Mohapatra (eds.), Computational Intelligence in Data Mining—Volume 2, Advances in Intelligent System and Computing, 2017; 411, DOI 10.1007/978-81-322-2731-1_37

10. Ying-Chih Wu, Wei-Ping Lee, Ching-Wei Chien "Modified the Performance of Differential Evolution Algorithm with Dual Evolution Strategy" International Conference on Machine Learning and Computing IPCSIT, 2011; 3 © (2011) IACSIT Press, Singapore
11. H. Golpîra, H. Bevrani ―Application of GA optimization for automatic generation control design in an interconnected power system‖ Energy Conversion and Management, 2018; 52: 2247–2255.
12. E.S. Ali, S. M. Abd-Elazim ― BFOA based design of PID controller for two area Load Frequency Control with nonlinearities" E.S. Ali, S.M. Abd-Elazim/Electrical Power and Energy Systems, 2016; 33: 633–638.
13. B. Padmanabhan, R.S. Sivakumar, J. Jasper and T. Aruldoss Albert Victoire ―Bacterial Foraging Approach to Economic Load Dispatch Problem with Non Convex Cost Function" B.K. Panigrahi et al. (Eds.): SEMCCO, Part I, LNCS, 2011; 7076: 577–584.
14. Kamel Sabahia and Easa Narimania and ahmad faramarzi ―Dynamic Neural Network for AGC in Restructure Power System‖ 2010 IEEE International Conference on Power and Energy (PECon2010), Kuala Lumpur, Malaysi, 2010; 29: 1.
15. Praghnesh Bhatt, Ranjit Roy *, S.P. Ghoshal ―Optimized multi area AGC simulation in restructured power systems‖ Electrical Power and Energy Systems, 2010; 32: 311–322.
16. Muwaffaq Irsheid Alomoush "Load frequency control and automatic generation control using fractional-order controllers" Electr Eng, 2017; 91: 357–368. DOI 10.1007/s00202-009-0145-7
17. Susanta Dutta, Sourav Paul, Kuntal Bhattacharjee, Aniruddha Bhattacharya, Roy Ranadhir Sarkar ―. Automatic generation control of an interconnected hydro-thermal system with thyristor control phase shifter using gravitational search algorithm" Advances in Engineering, Science and Management (ICAESM), 2012 International Conference on, 2012; 30-31, 269 – 274.
18. Solai, baghya shree & Kamaraj, Nagappan. Hybrid Neuro Fuzzy Controller for Automatic Generation Control of Multi Area Deregulated Power System. Circuits and Systems, 2016; 07: 292-306. 10.4236/cs.2016.74026.

19. Parmar, K.P.S., Majhi, S. and Kothari, D.P. 'LFC of an interconnected power system with multi-source power generation in deregulated power environment', International Journal Electric Power Energy Systems, 2014; 57: 277–286.
20. Gorripotu, T.S., Sahu, R.K. and Panda, S. 'AGC of a multi-area power system under deregulated environment using redox flow batteries and interline power flow controller', International Journal Engineering Science and Technology, 2015; 18, 4: 555–578.
21. Babu, A.S. and Saibabu, C.H. 'Simulation studies on automatic generation control in deregulated environment without considering GRC', International Journal of Engineering Science and Technology, March, 2012; 4, 3: 912–921.
22. Kumar, P., Kazmi, S.A. and Yasmeen, N. 'Comparative study of automatic generation control in traditional and deregulated power environment', World Journal of Modeling and Simulation, 2010; 6, 3: 189–197.